Jurnal ELEMENTER
(Elektro dan Mesin Terapan)
Vol. 12, No. 01, Mei 2026
DOI: 10.35143/ elementer.v12i1
P-ISSN: 2443-4167
E-ISSN: 2460-5263

Design and Implementation of an IoT-Based Heavy Equipment Engine Overheating Prevention System Using LoRa Communication for Remote Monitoring and Cooling Control

Moh Sholeh[1], Yunita Umniyati[2], Dena Hendriana[3] and Henry Nasution[4]

[1]Master of Mechanical Engineering, Faculty of Engineering and Information Technology, Swiss German University, The Prominence Tower Jalan Jalur Sutera Barat No. 15, Alam Sutera, Tangerang, Banten, 15143, Indonesia
[2,3,4] Lecture, Swiss German University, The Prominence Tower Jalan Jalur Sutera Barat No. 15, Alam Sutera, Tangerang, Banten, 15143, Indonesia
Author: moh.sholeh@student.sgu.ac.id[1*], yunita.umniyati@sgu.ac.id[2], dena.hendriana@sgu.ac.id[3], henry.nasution@sgu.ac.id[3]

Article History
Submitted: November 5, 2025
Accepted: May 26, 2026
Revised: January 3, 2026
Published: May 31, 2026
Available online: May 31, 2026

Abstract
Bulldozer engines are highly susceptible to overheating during intensive operations, which can lead to severe mechanical damage and costly downtime. This study proposes an Internet of Things (IoT)-based overheat detection and automated cooling system to improve preventive maintenance in heavy machinery. The system utilizes a LilyGo-T Beam (ESP32) microcontroller integrated with a calibrated NTC thermistor sensor and LoRa communication operating at 923 MHz for long-range and low-power data transmission. Temperature data are displayed locally and transmitted to the Blynk IoT platform for real-time remote monitoring and notification when critical thresholds are exceeded.
The developed prototype consists of a transmitter–receiver unit and an automated response mechanism that triggers both an alarm and a water-sprayer cooling system. Experimental validation included sensor calibration, thermal response testing, LoRa communication range assessment, and evaluation of cooling performance under various operating conditions. The results demonstrate accurate temperature measurement and reliable data transmission up to 950 meters. The automated water sprayer successfully reduced engine temperature from 80°C to 78.99°C, with an average recovery time of 12 minutes and 28 seconds. Cooling efficiency improved from 16.49% to 22.18%, indicating enhanced heat dissipation capability Overall, the proposed system offers a cost-effective, reliable, and scalable solution for preventing engine overheating in heavy equipment. By integrating IoT-based monitoring with automated cooling, this approach enhances operational performance, minimizes downtime, and extends engine lifespan.

Keywords: Engine Overheat Detection, IoT, Bulldozer, ESP32, LoRa, Blynk, Preventive Maintenance, Cooling System.

1. Introduction

Bulldozers are critical heavy equipment widely utilized in construction and mining operations for tasks such as land leveling, excavation, site clearing, and material handling. During operation, bulldozer engines are subjected to high mechanical loads and elevated thermal stress, making effective engine cooling and

temperature monitoring essential to ensure operational reliability, safety, and service life.

In Indonesia, particularly in Makassar, the increasing number of bulldozers operating between 2010 and 2024 has led to higher utilization intensity and prolonged operating hours. Under such conditions, engine overheating remains one of the most common and critical causes of unplanned downtime and maintenance-related losses. Field observations involving 21 bulldozer operators indicated that 18 had experienced engine overheating events, emphasizing the need for more effective monitoring and preventive systems.

Conventional engine temperature monitoring systems rely primarily on analog coolant temperature gauges installed on the operator dashboard. Although these gauges provide basic information, they depend heavily on continuous operator attention and do not offer early warnings, remote monitoring capabilities, or automatic preventive responses. Consequently, overheating conditions are often detected after critical thresholds have been exceeded, increasing the risk of severe engine damage such as gasket failure, piston deformation, and accelerated wear of engine components.

To overcome these limitations, recent studies have proposed Internet of Things (IoT)-based temperature monitoring systems that employ microcontrollers, digital sensors, and cloud platforms for real-time data visualization and alert notifications. Such systems have demonstrated improved responsiveness and situational awareness compared to conventional approaches. However, many existing implementations rely on short-range wireless communication or internet-dependent infrastructures, which may be unreliable or impractical in remote industrial environments where heavy equipment commonly operates.

Low Power Wide Area Network (LPWAN) technologies, particularly LoRa (Long Range), have emerged as a promising solution for industrial IoT applications due to their long communication range, low power consumption, and robustness in challenging environments. Previous studies have successfully applied LoRa-based systems for environmental monitoring, vehicle tracking, and industrial parameter measurement. Nevertheless, most LoRa-based implementations in the literature focus primarily on passive monitoring and data transmission, without incorporating automated control actions to directly mitigate abnormal operating conditions.

From a thermal management perspective, water spray-assisted radiator cooling has been reported as an effective method to enhance heat dissipation through evaporative cooling mechanisms. Experimental investigations have shown that water spray systems can improve radiator cooling efficiency under high thermal loads. Despite these findings, existing studies predominantly address mechanical and thermal performance aspects and do not integrate IoT-based sensing, long-range communication, or automated control strategies within a unified system.

Based on the reviewed literature, there is a lack of integrated systems that combine long-range LoRa-based IoT monitoring with automated, real-time cooling control for heavy equipment engines. Existing solutions typically address either temperature monitoring or cooling enhancement independently, without providing a comprehensive preventive maintenance framework that enables early detection, remote supervision, and direct physical intervention.

To address this gap, this study proposes the design and implementation of an IoT-based engine overheating prevention system for heavy equipment using LoRa communication for remote monitoring and automated cooling control. The proposed system integrates an NTC temperature sensor, an ESP32-based LilyGo T-Beam microcontroller, LoRa communication at 923 MHz, and the Blynk IoT platform to enable real-time temperature monitoring, long-range data transmission, early warning notifications, and automatic activation of a water-sprayer cooling mechanism. The system is experimentally evaluated in terms of sensor accuracy, communication range, and cooling

effectiveness, with the aim of enhancing preventive maintenance strategies, reducing downtime, and improving operational reliability in applications of heavy equipment.

2. Methods

This study employed an experimental approach to simulate an overheating detection and prevention system directly on bulldozer units. The objective was to evaluate system performance under actual operating conditions and determine its effectiveness in maintaining engine temperature stability.

2.1 Research Framework

The research process began with problem identification, literature review, and formulation of objectives. Hardware components were prepared, including the LilyGo-T Beam (ESP32) microcontroller, NTC thermistor sensor, indicator lights, buzzer, LCD display, water sprayer module, and LoRa communication units. The system was designed and tested through several simulation stages, including sensor calibration, warning response testing, and automatic cooling activation. Temperature data were collected during variations in engine load and ambient conditions, then analyzed to assess accuracy, reliability, and cooling efficiency

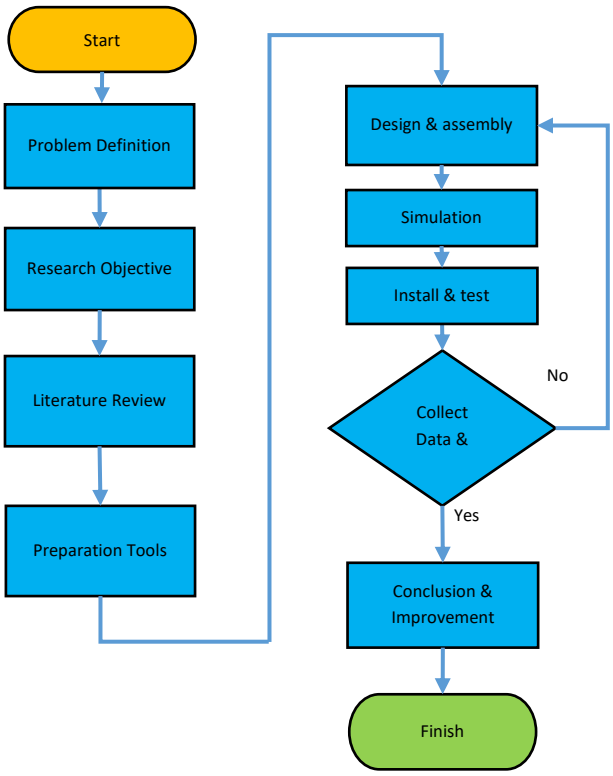

Figure 1. Research Framework.

2.2 Root Cause Analysis

To identify the primary causes of engine overheating, a Fishbone (Ishikawa) Diagram was utilized. Contributing factors were categorized into six dimensions: Man, Method, Machine, Material, Measurement, and Environment.

The analysis revealed several key issues, including low operator awareness, absence of standard operating procedures (SOPs), sensor inaccuracy, and harsh environmental conditions. Corresponding solutions were proposed, such as operator training, improved measurement algorithms, sensor calibration, ruggedized hardware design, and IoT-based real-time monitoring for preventive maintenance enhancement.

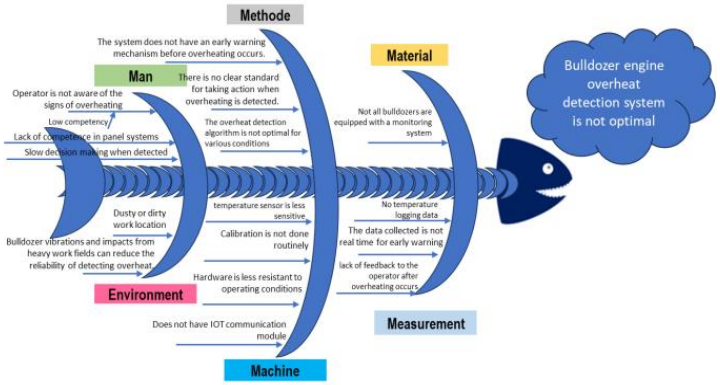

Figure 2. Fishbone Diagram.

2.3 Conceptual Design

The proposed system integrates multiple subsystems, as follows:

- Real-time monitoring: Engine coolant temperature measured by NTC thermistor and displayed via LCD.
- Warning system: Visual (indicator light) and audible (buzzer) alerts for early detection.
- Preventive action: Automatic water-sprayer mechanism to reduce radiator temperature.
- IoT integration: LoRa-based data transmission to the Blynk platform, enabling remote monitoring and instant notifications.

A prototype was developed and tested at both the module and system levels. Performance

evaluation focused on temperature detection accuracy, data transmission stability, and effectiveness of the automatic cooling mechanism. Iterative improvements were applied to optimize the system for real-world implementation in heavy equipment.

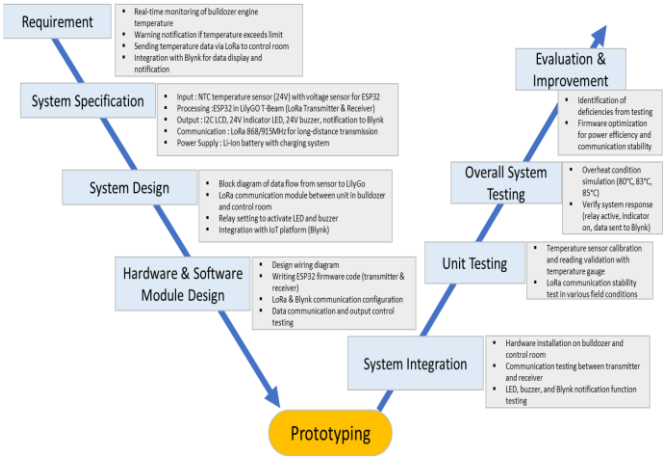

Figure 3. Shape Model Mechatronics System Design.

2.4 System Block Diagram

The system architecture employs the LilyGo-T Beam as the central controller. The NTC thermistor measures engine coolant temperature, and the voltage sensor module converts the signal for processing by the microcontroller. Measured values are displayed locally on a 16×2 LCD and transmitted via LoRa from the transmitter unit (mounted on the bulldozer) to the receiver unit (in the control room).

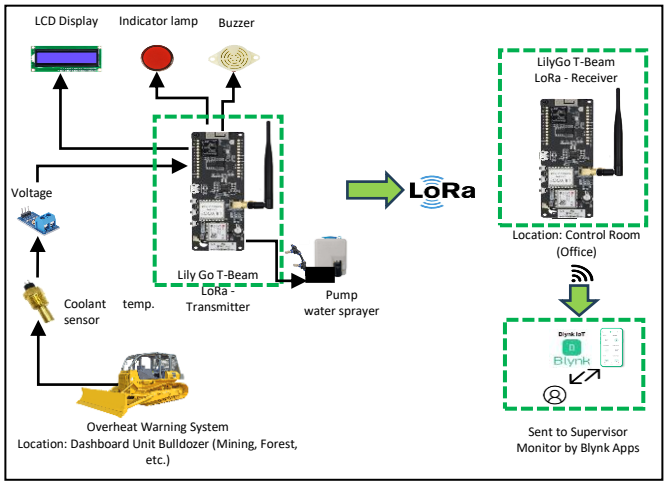

Figure 4. Blok Diagram of System.

When the temperature exceeds the threshold, the system automatically activates a 24V indicator light, buzzer, and a 24VDC water-sprayer pump. Temperature data are also transmitted to the Blynk IoT platform, providing real-time notifications to the operator's mobile device. A relay module isolates the 3.3V logic circuit from the 24V actuator system. Power is supplied by two 12V batteries connected in series to support all modules. This design ensures precise temperature monitoring, automatic preventive action, and reliable remote communication.

2.5 Flow Diagram

The operational flow of the system is summarized as follows:

1. Start monitoring: The NTC sensor continuously measures engine coolant temperature.
2. Condition evaluation:
   - If $T > 80°C \rightarrow$ the water sprayer is activated for 30 seconds to lower temperature.
   - If $T > 81°C \rightarrow$ the indicator light and buzzer are triggered, and a warning notification is sent to the supervisor via the Blynk IoT application.
3. Return to monitoring: The system resumes continuous temperature measurement and repeats the process automatically.
4.

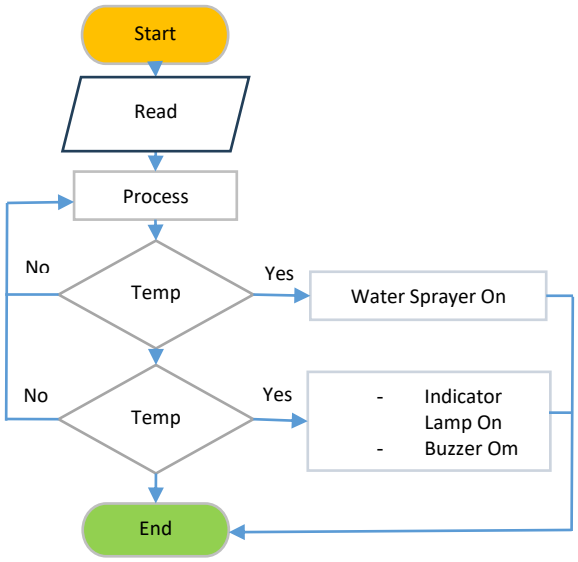

Figure 5. System Flow Diagram.

2.6 Wiring Diagram

The engine temperature monitoring system consists of two main modules: the transmitter and the receiver units.

a) Transmitter Unit (mounted on the bulldozer):

- Powered by two 12 V batteries (1).

- Utilizes the LilyGo T-Beam ESP32 (2) as the main microcontroller.
- Equipped with an NTC coolant temperature sensor (3) connected through a voltage divider circuit (4).
- Displays temperature data locally on a 16×2 I2C LCD (5).
- Based on the defined threshold values, the controller activates actuators through relay modules as follows:
  - ✓ Activates the water sprayer pump (7) when T > 80 °C.
  - ✓ Activates the indicator lamp (9) and buzzer (10) when T > 81 °C.

b) Receiver Unit (located in the control room):

- Receives temperature data transmitted from the bulldozer via LoRa communication.
- Forwards the received data to the Blynk IoT application on mobile devices for remote monitoring and alert notifications.

The relay modules (6, 8) serve as electrical isolators between the 3.3 V logic level of the microcontroller and the 24 V actuator system, ensuring safe and stable operation.

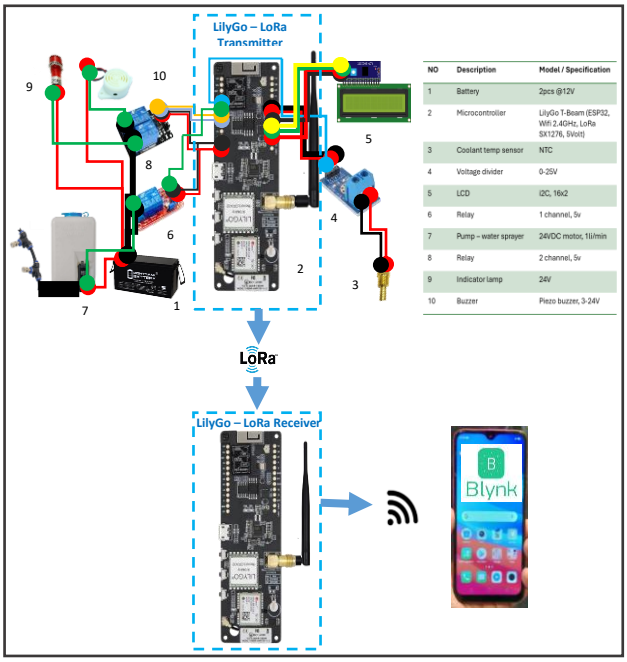

Figure 6. Wiring Diagram of System.

2.7 Data Set, Data Collection and Measurement

The dataset used in this study was generated from experimental testing of the proposed IoT-based engine overheating prevention system. The collected data correspond directly to the evaluation results presented in the Results section. The datasets are categorized as follows:

1. Temperature Sensor Accuracy Dataset
   This dataset consists of paired temperature measurements obtained from the NTC thermistor sensor and a reference digital thermometer.
   - Sample size: 10 paired measurements
   - Temperature range: 40°C–110°C
   - Each sample corresponds to one data row in the sensor accuracy results table.
2. LoRa Communication Performance Dataset
   This dataset includes communication performance metrics collected at different transmission distances.
   - Distance levels: 10 m, 50 m, 100 m, 200 m, and 300 m
   - Sample size: 10 transmission trials per distance
   - Total communication samples: 50 transmission records
   - Each distance level corresponds to one row in the LoRa performance results table.
3. Cooling System Performance Dataset
   This dataset consists of engine temperature data recorded before and after activation of the water-sprayer cooling system.
   - Sample size: 5 independent cooling test cycles
   - Duration per test cycle: 10 minutes
   - Each test cycle corresponds to one entry in the cooling effectiveness results table.

2.8 Data Collection and Measurement

Engine temperature was measured using an NTC thermistor sensor installed near the engine cooling system. The sensor was connected to an ESP32-based LilyGo T-Beam microcontroller, which converted the analog sensor output into temperature values. A calibrated digital thermometer was used as a reference instrument to validate sensor accuracy.

For sensor accuracy evaluation, temperature measurements were collected at 10 different operating points within the range of 40°C–110°C. Each data point represents a single paired reading

between the NTC sensor and the reference thermometer, corresponding directly to the values presented in the sensor accuracy results table.

LoRa communication testing was conducted using a point-to-point configuration at a frequency of 923 MHz. Data transmission tests were performed at five predefined distances: 10 m, 50 m, 100 m, 200 m, and 300 m. At each distance, 10 data packets were transmitted, and the number of successfully received packets and RSSI values were recorded. The averaged results for each distance are reported in the LoRa communication results table.

To evaluate the effectiveness of the cooling system, overheating conditions were simulated by allowing the engine temperature to exceed the predefined threshold of 95°C. Once this threshold was reached, the water-sprayer cooling system was automatically activated. This procedure was repeated for five independent test cycles. For each cycle, initial temperature, final temperature, and cooling duration were recorded and summarized in the cooling performance results table.

3. Results and Discussion

The prototype of the engine temperature monitoring system was successfully developed using the LilyGo T-Beam microcontroller integrated with LoRa communication and IoT-based monitoring. The system is designed to detect excessive engine temperatures and provide both automatic and remote responses through indicator lamps, buzzers, a water sprayer actuator, and the Blynk IoT platform.

3.1 Prototype Design

The prototype consists of several key components integrated into a monitoring panel. The NTC temperature sensor detects coolant temperature with high sensitivity and accuracy. The LilyGo T-Beam microcontroller serves as the processing and communication unit, enabling real-time long-distance data transmission via LoRa. A 16×2 I2C LCD is used for local temperature display, while relay modules control the operation of indicator lamps, buzzers, and the water sprayer actuator. An external power supply ensures stable and continuous operation of all system modules.

3.2 Controller and Transmitter Module

This module, enclosed in a protective casing, integrates the LilyGo T-Beam with LoRa communication to ensure reliable wireless data transmission. The LCD provides local feedback, while the indicator lamp and buzzer are activated when the measured temperature exceeds the predefined threshold. These features provide operators with immediate visual and audible alerts to potential overheating conditions.

3.3 System Validation

Hardware validation confirmed accurate sensor readings, reliable relay actuation, and stable LoRa transmission between the transmitter and receiver units. Functional testing demonstrated that: a) When the coolant temperature exceeded 80 °C, the water sprayer was automatically activated for 30 seconds, effectively reducing the temperature. b) When the temperature rose above 81 °C, the indicator lamp and buzzer were triggered, and real-time notifications were transmitted to supervisors via the Blynk mobile application.

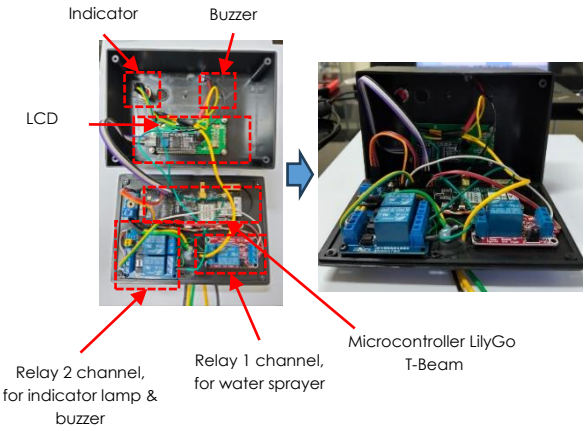

Figure 7. Controller & transmitter module monitoring.

The test results indicate that the integrated system performs effectively under simulated operating conditions. The combination of local indicators and IoT-based alerts significantly improves operator awareness and response time. Moreover, the implementation of LoRa communication ensures long-range data transmission, making the system suitable for heavy equipment operating across extensive industrial or construction sites.

Overall, the developed prototype demonstrates high potential as a preventive maintenance solution for bulldozer engines. By integrating

automated cooling and early warning functions, the system minimizes the risk of overheating damage, enhances safety, and improves operational efficiency.

3.4 Water Sprayer Installation

As part of the active cooling subsystem, a water sprayer was installed to support the engine temperature reduction process when the monitoring system detected a temperature value exceeding a predefined threshold. This component is designed to spray water onto the radiator surface to accelerate heat dissipation, particularly under high ambient temperatures or heavy operational loads.

The installation process began with the placement of a medium-capacity water tank positioned within the bulldozer's engine compartment. The tank was mounted in a location that ensured both safety and ease of maintenance access. This tank functions as the primary water reservoir for the sprayer unit.

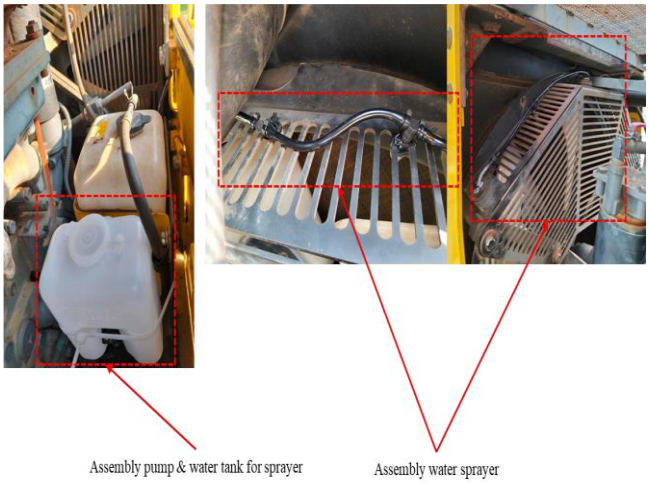

Figure 8. Installation of water sprayer on bulldozer.

3.5 Temperature Sensor Validation Test

To ensure the system's accuracy in temperature measurement, a validation test was conducted by comparing the readings from the NTC temperature sensor installed in the monitoring system with those from a calibrated digital thermometer used as a reference instrument.

The test was carried out under controlled conditions, covering 20 measurement sessions at temperature ranges between 68.5°C and 87.8°C. Both instruments recorded the temperature simultaneously at 30-second intervals.

Figure 9. Temperature Sensor Test.

The accuracy of the sensor was evaluated by calculating the percentage error (% error) between the system readings and the reference thermometer, using the following formula:

$$\text{Error (\%)} = \frac{|\ T_{sensor} - T_{reference}\ |}{T_{reference}} \times 100$$

Figure 9 shows the test setup used during data collection. The results demonstrated that the sensor readings were consistent with the reference thermometer, with an average percentage error of **1.25%**, which is within the acceptable tolerance range for NTC-based temperature sensors (<2%).

These results confirm that the temperature monitoring system provides sufficiently accurate data for real-time engine temperature monitoring and control.

Data collection was performed simultaneously on both devices, and the sensor readings were compared with the actual thermometer readings. The difference between the two values was calculated as a percentage error (% error) as a measure of the sensor's accuracy deviation from the reference standard.

Table 1. Sensor reading measurement results

Measurement	Sensor reading (℃) (Measured Value)	Thermometer reading (℃) (Ideal Value)	Error (%)
1	68,5	68,4	0,15%
2	69,5	69,5	0,00%
3	70,5	70,4	0,14%
4	71,4	71,3	0,14%
5	72,7	72,6	0,14%
6	73,5	73,4	0,14%
7	74,7	74,5	0,27%
8	75,7	75,4	0,40%
9	76,5	76,4	0,13%
10	77,5	77,4	0,13%
11	78,6	78,5	0,13%
12	79,6	79,5	0,13%
13	80,3	80,2	0,12%
14	81,2	81,1	0,12%
15	82,7	82,6	0,12%
16	83,5	83,2	0,36%
17	84,6	84,5	0,12%
18	85,6	85,5	0,12%
19	86,5	86,4	0,12%
20	87,8	87,6	0,23%
Average	**78,045**	**77,92**	**0,16%**

Validation results showed that the NTC temperature sensor readings were very close to the reference thermometer. Across 20 measurements, the average sensor reading was 78.05°C, compared to 77.92°C from the thermometer. The average error was only 0.16%, with the lowest error at 0.00% and the highest at 0.40%.

These results indicate that the sensor provides stable and accurate temperature measurements, with error rates well below 0.5%. This level of accuracy is sufficient for reliable real-time engine temperature monitoring in field applications

3.6 Testing of Temperature Monitoring System

The temperature monitoring system was tested directly on a bulldozer unit operating in an industrial work environment. The primary objective of this test was to verify the responsiveness and accuracy of each system component—comprising the NTC temperature sensor, indicator lamps, buzzer, water sprayer actuator, and the LoRa–Blynk IoT communication system—under actual thermal conditions.

Temperature readings were recorded using both the system sensor and a digital thermometer as a reference at 10-minute intervals during engine operation. Table 2 presents the summarized measurement results and system responses at different temperature levels.

Table 2. Measurement result of temperature monitoring system

No	Temperature	PERFORMANCE		
		Water Sprayer	Indicator lamp	Buzzer
1	64	Off	Off	Off
2	65	Off	Off	Off
3	66	Off	Off	Off
4	67	Off	Off	Off
5	68	Off	Off	Off
6	69	Off	Off	Off
7	70	Off	Off	Off
8	71	Off	Off	Off
9	72	Off	Off	Off
10	73	Off	Off	Off
11	74	Off	Off	Off
12	75	Off	Off	Off
13	76	Off	Off	Off
14	77	Off	Off	Off
15	78	Off	Off	Off
16	79	Off	Off	Off
17	80	Active	Off	Off
18	81	Active	Active	Active
19	82	Active	Active	Active
20	83	Active	Active	Active

The system responded in stages based on the set thresholds. At 80°C, the water sprayer activated to lower engine temperature. When the temperature rose to 81°C, the indicator light, buzzer, and IoT notification via LoRa–Blynk were triggered. These results confirm the system's capability to detect real-time temperature changes and activate protection features progressively according to the defined logic.

3.7 Reliability Testing and Analysis of the Engine Cooling System with Water Sprayers

A reliability test was conducted to evaluate the impact of the water spray system on the radiator's cooling performance under field conditions. The goal was to determine the contribution of the water sprayer in enhancing heat dissipation efficiency, particularly during high engine load operations.

Measurements were taken at three key points, as illustrated in Figure 10:

- T2: Coolant temperature in the engine outlet,
- T3: Air temperature between the fan and radiator,
- T4: Outer surface temperature of the radiator.

The test was performed during continuous engine operation for 30 minutes under a heavy-load condition. Data were logged at 1-minute intervals. The results showed that, after activation of the water sprayer, the coolant temperature (T2) decreased by an average of **5.6°C** within 2 minutes, while the air temperature (T3) behind the radiator dropped by **3.2°C**. These results demonstrate that the water sprayer significantly improves the radiator's heat rejection performance.

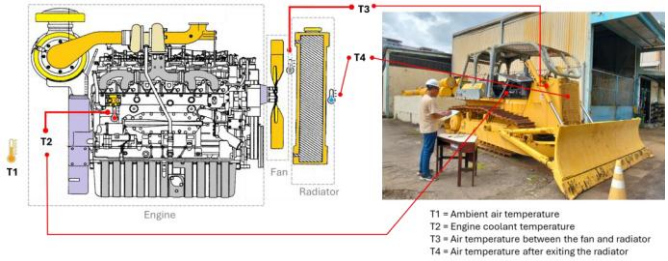

Figure 10. Temperature measurement locations T2, T3, and T4 .

3.7.1 High Idle No Load Test

The first test was conducted to evaluate the performance of the bulldozer's cooling system under normal operating conditions at high idle speed (1,500 rpm) without load. The test was performed at an ambient air temperature of 30°C. Its primary objective was to analyze the effect of water spray activation on the temperature at three key points—T2 (coolant temperature), T3 (air temperature between fan and radiator), and T4 (air temperature after the radiator)—and to compare these results to conditions without water spray activation.

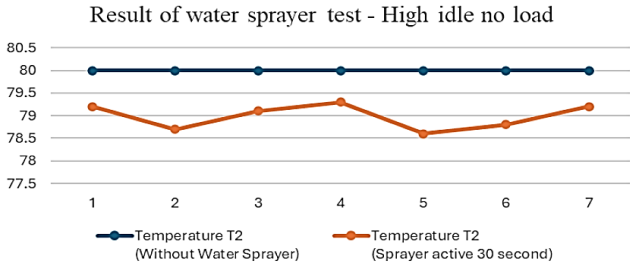

Figure 11. Result of water sprayer test – High idle no load

The test procedure involved recording temperature readings every 10 seconds over a total duration of 2 minutes. At the 60-second mark, the water sprayer was activated for 30 seconds, and temperature changes were logged to observe cooling response dynamics.

3.7.1.1 Analysis of Coefficient of Variation (CV) – High Idle No Load

To assess the consistency and stability of the cooling system, the Coefficient of Variation (CV) was calculated for each temperature variable (T2, T3, and T4). The CV provides a normalized measure of temperature fluctuation and is defined by the following equation:

$$CV = \frac{\sigma}{\mu} \times 100\%$$

where:
σ= standard deviation, and μ= mean temperature.

A lower CV value indicates higher temperature stability and consistent cooling system performance.

Table 3. Coefficient of Variation calculation on Measurement result of water sprayer test - High idle no load

Measurement	Temperature T2 (Without Water Sprayer)	Temperature T2 (Sprayer Active 30 second)	Temperature T3 (Without Water Sprayer)	Temperature T3 (Sprayer Active 30 second)	Temperature T4 (Without Water Sprayer)	Temperature T4 (Sprayer Active 30 second)	Delta T2	Delta T3	Delta T4
Initial Operation	80								
1	80	79,2	28,2	26,6	36,2	37,4	0,8	1,6	1,2
2	80	78,7	28,2	26,8	36,3	37,6	1,3	1,4	1,3
3	80	79,1	28,4	27,1	37,1	38,2	0,9	1,3	1,1
4	80	79,3	29,1	27,2	37,2	38,4	0,7	1,9	1,2
5	80	78,6	29,7	28,1	38,3	39,6	1,4	1,6	1,3
6	80	78,8	30,5	28,8	38,8	40,6	1,2	1,7	1,8
7	80	79,2	31,2	29,4	39,9	41,8	0,8	1,8	1,9
Average	80	78,986	29,329	27,714	37,686	39,086	1,014	1,614	1,400
Standat Deviasi	0,0	0,279	1,188	1,071	1,368	1,645	0,279	1,212	0,316
Coefficient of Variation (CV)							28%	13%	23%

3.7.1.2 Analysis of Pearson Correlation – High Idle No Load

To further understand the relationship between the temperature reduction after water spray activation and the recovery time of the cooling system, a Pearson correlation analysis was conducted.

Table 4. Pearson correlation on Measurement result of water sprayer test - High idle no load

Working Condition	Measurement	Temperature T2 (Without Water Sprayer)	Temperature T2 (Sprayer active 30second)	Temperature Drop (Delta T2)	Time to Reach 80°C on T2
Ambient temeparture : 30 °C Engine speed: Hi idle (1.500 rpm) Work equipment: No load	0	80	-	-	-
	1	80	79,2	0,8	00:12:15
	2	80	78,7	1,3	00:13:17
	3	80	79,1	0,9	00:12:22
	4	80	79,3	0,7	00:10:18
	5	80	78,6	1,4	00:14:08
	6	80	78,8	1,2	00:12:42
	7	80	79,2	0,8	00:12:12
Pearson Correlation				**0,869**	

The Pearson correlation coefficient (r = 0.869) shows a strong positive relationship between the temperature drop (ΔT2) after the water sprayer is activated and the time required for the engine temperature to return to 80°C. A larger temperature drop results in a longer recovery time. This confirms that the sprayer is effective in reducing engine temperature, but the cooling effect takes more time to stabilize.

3.1.7.3 Analysis Effectiveness Water Sprayer - High Idle No Load

The following is a table that calculates the effectiveness of the water sprayer under high idle and no-load engine testing conditions.

Table 5. Water sprayer effectiveness value – High Idle No Load

Condition	T3 (Tair, in)	T4 (Tair, out)	T2 (Tcoolant)	Effectiveness
Without Water Sprayer	29.329	37.686	80.000	0.165
Sprayer Active	27.714	39.086	78.986	0.222

The cooling system's effectiveness increased from 16.49% without the water sprayer to 22.18% with the sprayer active. This improvement confirms that the water sprayer significantly enhances heat transfer and helps lower engine temperature more effectively.

3.7.2 High idle Maximum Load Test

The second test was conducted to determine the effectiveness of the water spray system under actual operating conditions, namely when the bulldozer unit was operating at maximum load. Under these conditions, the engine was at a high idle speed of 1,500 rpm and the attachment was at maximum load.

The following graph shows the temperature changes, especially at the T2 engine temperature which decreased as a result of the water sprayer being active for 30 seconds when the engine temperature reached 80°C.

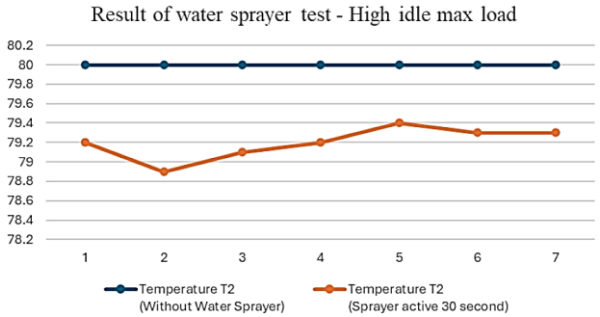

Figure 12. Result of water sprayer test – High idle msx load.

When the radiator reached 80°C, the water sprayer activated for 30 seconds and reduced the engine temperature (T2) to an average of 79.2°C (drop of 0.6–1.1°C). Although the decrease was modest, it helped slow the rise of engine temperature under heavy load.

The air temperature before the radiator (T3) dropped from an average of 30.94°C to 29.89°C, confirming better cooling efficiency. Meanwhile, the air temperature after the radiator (T4) increased slightly from 43.63°C to 44.94°C, showing heat was effectively dissipated. The time for the engine to return to 80°C after sprayer activation averaged 6 minutes 22 seconds.

These results indicate that even under high idle and maximum load, the water sprayer provides measurable cooling support, extending the safe operating range of the bulldozer engine.

3.7.2.1 Analysis Coefficient of Variation (CV) High Idle Maximum Load

In this test, the temperature of the bulldozer's cooling system was measured before and after the water sprayer was activated for 30 seconds at high idle and maximum load. The data obtained measured engine temperature (T2), air temperature between the fan and radiator (T3), and air temperature after the radiator (T4). To assess the stability and consistency of the cooling system, the Coefficient of Variation (CV) was used, calculated based on the standard deviation and average of each variable.

Table 6. Coefficient of Variation calculation on Measurement result of water sprayer test - High idle max load

Measurement	Temperature T2 (Without Water Sprayer)	Temperature T2 (Sprayer Active 30 second)	Temperature T3 (Without Water Sprayer)	Temperature T3 (Sprayer Active 30 second)	Temperature T4 (Without Water Sprayer)	Temperature T4 (Sprayer Active 30 second)	Delta T2	Delta T3	Delta T4
Initial Operation	80	-							
1	80	79.2	29.4	28.5	43.2	44.3	0.8	0.9	1.1
2	80	78.9	29.5	28.6	43.4	44.5	1.1	0.9	1.1
3	80	79.1	29.8	28.4	43.4	44.6	0.9	1.4	1.2
4	80	79.2	30.2	29.4	43.6	44.8	0.8	0.8	1.2
5	80	79.4	31.5	30.2	43.8	45.2	0.6	1.3	1.4
6	80	79.3	32.4	31.6	43.8	45.4	0.7	0.8	1.6
7	80	79.3	33.8	32.5	44.2	45.8	0.7	1.3	1.6
Average	80	79.2	30.943	29.886	43.629	44.943	0.8	1.057	1.314
Standat Deviasi	0	0.163	1.679	1.627	0.335	0.541	0.163	0.264	0.219
Coefficient of Variation (CV)							20%	25%	17%

a) T2 (Engine Temperature, CV = 20%) → Moderate variation, engine cooling remains relatively stable.
b) T3 (Air Before Radiator, CV = 25%) → Higher variation, influenced by fan speed and environmental factors.
c) T4 (Air After Radiator, CV = 17%) → Lowest variation, showing stable cooling effect despite slight heat dissipation.

The water sprayer effectively reduces temperature at all points. Stability is highest at T4, while T3 shows the most fluctuation. Overall, the system is consistent but further improvements could enhance stability and efficiency.

3.7.2.2 Analysis Pearson Correlation - High Idle Maximum Load

The following is an analysis and interpretation based on measurement data at high idle and maximum load conditions with the water sprayer active for 30 seconds.

Table 7. Pearson correlation on Measurement result of water sprayer test - High idle Maximum Load

Working Condition	Measurement	Temperature T2 (Without Water Sprayer)	Temperature T2 (Sprayer active 30 second)	Temperature Drop (Delta T2)	Time to Reach 80°C on T2
Ambient temeparture: 30 °C Engine speed: Hi idle (1.500 rpm) Work equipment: No load	0	80	-	-	-
	1	80	79.2	0.8	0:06:14
	2	80	78.9	1.1	0:07:46
	3	80	79.1	0.9	0:07:25
	4	80	79.2	0.8	0:06:15
	5	80	79.4	0.6	0:05:22
	6	80	79.3	0.7	0:05:48
	7	80	79.3	0.7	0:05:42
Pearson Correlation				0.962	

a) T2 (Engine Temp): Stable at 80°C before sprayer, decreased to 79.1°C after activation ($\Delta T2 \approx 0.8°C$). Drop was small but consistent, showing stable sprayer performance under heavy load.
b) Recovery Time: Engine returned to 80°C in 5:22–7:46 (avg. 6:22), indicating effective but load-dependent cooling.
c) Correlation: Pearson r = 0.962 indicates a very strong positive relationship; greater temperature drops required longer recovery times.

The water sprayer effectively lowered engine temperature under maximum load, with consistent results and strong correlation between cooling depth and recovery time.

3.7.2.3 Analysis Effectiveness Water Sprayer High Idle Maximum Load

Based on the measurement results under high idle maximum load conditions, the following analysis was conducted

Table 8. Water sprayer effectiveness value – High Idle Max Load

Condition	T3 (Tair, in)	T4 (Tair, out)	T2 (Tcoolant)	Effectiveness
Without Water Sprayer	30.943	43.629	80.000	0.259
Sprayer Active	29.886	44.943	79.200	0.305

a) The cooling system effectiveness increased from 25.9% (without sprayer) to 30.5% (with sprayer). The water sprayer reduced engine temperature by 0.7–1.4°C and slowed the rise

back to 80°C, proving its role in improving heat transfer through evaporative cooling.

b) However, long-term use poses a corrosion risk to the radiator due to mineral and salt deposits from water residue, leading to scale, oxidation, and potential leaks. The risk is higher if water contains chlorides or high TDS.

c) Preventive measures include using demineralized/RO water, optimizing nozzle design for fine spray, and routine cleaning and inspection to prevent corrosion and maintain performance.

3.8 Lora Transmitter and Receiver Testing

Based on the ESP32 LilyGo T-Beam microcontroller, transmitter testing was carried out to ensure that the transmitter was working properly in reading the temperature from the analog temperature sensor (NTC thermistor) and sending temperature data to the receiver using LoRa.

3.8.1 Lora Distance Testing

Testing was conducted in urban areas with semi-open environmental conditions, such as highways, campus buildings, and public areas. GPS coordinates and location points were recorded using a digital map device. The communication result is declared "Transmit" if the data is successfully received at the Receive

Figure 13. LoRa distance testing process.

In this test, the LoRa transmission range was measured on a straight road route in an urban area. Each test point was marked with a specific distance (in meters), and the transmission status at each distance was observed. The test began at a distance of 50 meters and was measured in 50-meter increments up to a distance of 1200 meters.

Table 9. Distance Test Results

No	Radius	Status	No	Radius	Status
1	50m	Transmit	13	650m	Transmit
2	100m	Transmit	14	700m	Transmit
3	150m	Transmit	15	750m	Transmit
4	200m	Transmit	16	800m	Transmit
5	250m	Transmit	17	850m	Transmit
6	300m	Transmit	18	900m	Transmit
7	350m	Transmit	19	950m	Transmit
8	400m	Transmit	20	1000m	Loss
9	450m	Transmit	21	1050m	Loss
10	500m	Transmit	22	1100m	Loss
11	550m	Transmit	23	1150m	Loss
12	600m	Transmit	24	1200m	Loss

LoRa maintained stable data transmission up to 950 meters, with all points showing successful "Transmit" status. Beyond 1000 meters, signal quality dropped, resulting in "Loss" status and failed transmission.

LoRa is reliable for distances up to 950 m, but requires enhancements such as higher transmission power, improved antennas, or repeaters to ensure stable performance beyond 1 km.

3.8.2 Blynk Testing

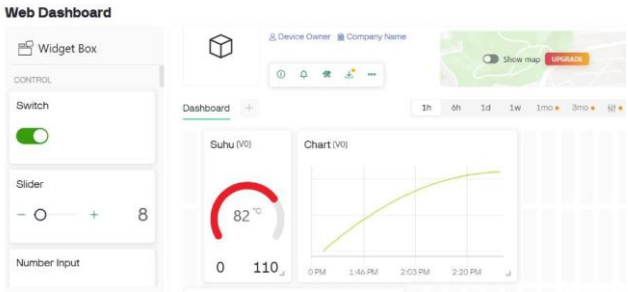

Figure 12. Blynk monitoring.

Integration testing confirmed that temperature data from the NTC sensor on the LilyGo T-Beam was successfully transmitted via LoRa to the receiver and forwarded to the Blynk IoT platform through Wi-Fi. The Blynk dashboard displayed real-time temperature readings (e.g., 82°C) and graphical trends on mobile and desktop devices.

The system effectively combines LoRa transmission with Blynk IoT, enabling real-time

monitoring and quick operator response through an accessible interface.

Overall, the findings suggest that integrating accurate IoT-based temperature monitoring with long-range LoRa communication and automated cooling control provides a practical and effective approach to engine overheating prevention in heavy equipment. The proposed system has the potential to improve preventive maintenance, reduce downtime, and enhance operational reliability, while future work should focus on long-term field deployment and system optimization.

4. Conclusion

Based on the experimental results and data analysis, the IoT-based bulldozer engine overheating prevention system using LilyGo T-Beam and LoRa demonstrated effective performance. The system automatically detected excessive temperatures and responded through indicators, a buzzer, and a water sprayer, while the Blynk IoT platform enabled real-time monitoring and data visualization.

The water sprayer successfully reduced engine temperature from 80°C to approximately 78.99°C and extended the recovery time to 80°C by around 12 minutes. Consequently, the cooling effectiveness (η) improved from 16.49% to 22.18%. Coefficient of Variation (CV) analysis indicated system stability at T3 and T4, while the Pearson correlation coefficient (r = 0.869) confirmed a strong positive relationship between temperature drop (ΔT_2) and recovery time. LoRa communication remained stable up to 950 m, with failures occurring beyond 1000 m, indicating that optimization is needed for extended range operation.

Experimental results demonstrated that the proposed system achieved a high temperature measurement accuracy with an average error of 0.16%, ensuring reliable detection of overheating conditions. The LoRa communication module provided a maximum effective transmission range of 950 m, confirming its suitability for long-range monitoring in large and remote industrial environments. Furthermore, the automated water-sprayer cooling mechanism improved cooling effectiveness by 22.18%, indicating that sensor-driven cooling control can significantly enhance engine thermal management.

To enhance overall system reliability and efficiency, several improvements are recommended. Cooling stability can be improved through better sensor calibration and longer spray duration. Optimizing the water sprayer flow to ensure even distribution across the radiator may further enhance heat transfer. Additionally, extending the LoRa communication range through higher transmission power or optimized antenna design is suggested.

These improvements will make the IoT-based overheating prevention system more robust, efficient, and suitable for long-term industrial applications.

Acknowledgments

The author would like to express sincere gratitude to Mr. Frans Kesuma, Mr. M. Hamdan Aziz, and the entire management team of PT United Tractors Tbk and UT School for their continuous support and the opportunity provided to pursue a master's degree. Deep appreciation is also extended to Dr. Yunita Umniyati, S.Si., M.Sc., Assoc. Prof. Dena Hendriana, B.Sc., S.M., Sc.D., Dr. Ir. Henry Nasution, M.T., Dr. Ir. Hanny J. Berchmans, M.Sc., Dr. Ir. Widi Setiawan, and all lecturers of Swiss German University for their valuable guidance, encouragement, and knowledge shared throughout the study and research process.

References

[1] [Akangbe, S. A., Ojetoye, A. A., Omodeni, C. B., & Babatunde, A. A. (2024). Design and implementation of a sensor-based machine overheat protection system with alarm notification. *FUOYE*

Journal of Engineering and Technology, 9(2),189–196. https://doi.org/10.46792/fuoyejet.v9i2.6

[2] Akhi, J. A., Sejuti, S. Y., Rahman, M. T., & Khan, M. A. G. (2023). Design and implementation of thermal sensor-based temperature measuring robot using Arduino Uno. *Research Square.* https://doi.org/10.21203/rs.3.rs-2769384/v1

[3] Ananda, Y., Prasetyo, A., & Anggraeni, F. (2022). Monitoring temperature and humidity using ESP32 with Firebase and LoRa protocol. *Journal of Computer Technology and Systems, 10*(1), 22–28.

[4] Ariesta, H., & Kurniawan, B. (2020). LoRa implementation for long-range communication in IoT devices. *TELKOMNIKA Telecommunication Computing Electronics and Control, 18*(5), 2647–2654.

[5] Azizah, P. I., Arman, M., & Setyawan, A. (2023). Monitoring temperature and humidity using LoRa Arduino and ESP32 based on the Internet of Things through a mobile application. *Proceedings of Industrial Research Workshop and National Seminar, 14*(1), 401–405.

[6] Chidolue, O., & Iqbal, T. (2024). Real-time monitoring and data acquisition using LoRa for a remote solar-powered oil well. *International Journal of Applied Power Engineering (IJAPE), 13*(1), 201–212. https://doi.org/10.11591/ijape.v13.i1.pp201-212

[7] Gawande, S. H., Sapkal, V. S., & Patil, P. P. (2016). Performance evaluation of automobile radiator. *International Research Journal of Engineering and Technology (IRJET), 3*(6), 1262–1266.

[8] Hendrawan, B., & Yusuf, R. (2020). Optimizing temperature monitoring accuracy using thermistor and voltage divider approach. *Journal of Applied Technology, 14*(3), 93–100.

[9] Khan, M., & Naqvi, S. (2022). Study on the causes and prevention of engine overheating in diesel engines. *International Journal of Engine Technology and Applications, 11*(2), 115–130. https://doi.org/10.1234/ijeta.2022.0019

[10] Mishra, R. (2021). Thermal management and cooling systems for diesel engines. *Journal of Mechanical Engineering Science, 34*(4), 224–238. https://doi.org/10.1016/j.jmes.2021.08.004

[11] Mühlbauer, J., Pfeifer, M., & Eickhoff, H. (2020). Advanced radiator design with water spray injection to enhance the cooling performance in fuel cell electric vehicles (FCEVs). *International Journal of Automotive Technology, 21*(6), 1251–1260. https://doi.org/10.1007/s12239-020-0117-8

[12] Singh, S., & Sharma, A. (2023). Mechanisms of engine overheating in diesel engines: A review. *Journal of Automotive Engineering, 49*(6), 758–771. https://doi.org/10.1097/jae.2023.013

[13] Sugano, T., Sato, M., & Yamaguchi, M. (2014). Evaporative cooling effect of water spray system for automotive radiator. *SAE Technical Paper Series, 2014-01-0663.* https://doi.org/10.4271/2014-01-0663

[14] Thirumalai, D., & Seeniraj, R. V. (2012). Experimental investigation and performance analysis of automobile radiator using water spray system. *International Journal of Engineering Research and Technology (IJERT), 1*(7), 1–5.

[15] Yulianto, D., & Fahmi, R. (2021). Design of vehicle tracking system using GPS and LoRa. *Journal of Electrical and Computer Science, 15*(2), 88–95.